Tunable optical fiber cascade filter by magneto-optical effect

Shahad I Younus (140178@student.uotechnology.edu.iq)
University of Technology
Anwaar A Al-Dergazly
Al-Nahrain University
A K Abass
University of Technology

Research Article

Keywords: cascade optical fiber, finite element method, multimode interference, magneto-optical effect

Posted Date: July 7th, 2021

DOI: https://doi.org/10.21203/rs.3.rs-669379/v1

Tunable optical fiber cascade filter by magneto-optical effect

Shahad I Younus[1], Anwaar A Al-Dergazly[2] and A K Abass [1]

Abstract

Optical filters based on cascade single mode - multimode - single mode fiber structure (SMS) has considerable attention as a reliable optical device the reliability is due to its simplicity, compactness, low cost, all fiber device, low transmission loss, and can be continuously tune the laser wavelength at a specific spectral range. The principle of the operation is based on self- image and multimode interference (MMI) phenomena. A tunable filter was simulated based on cascade single mode-no core-single mode (SNS) fiber structure surrounded by magneto-optical fluid (MOF) using finite element method (FEM), the influence of the no core fiber (NCF) diameter and length on the tunablility and the bandwidth is investigated and optimized. Two materials were adopted as a MOF. The results show that the tunability of the filter can be improved by decreasing the NCF diameter. A continuous wavelength tunability about 37 nm from 1518 to 1555 nm with a bandwidth about 10 nm is obtained. The device is highly stable, inexpensive, provide wide tuning range compared with other tuning methods. This device can be used in optical communication, fiber sensor, spectroscopy, and in fiber laser technology. To the best of our knowledge, this is the first optical fiber MMI tunable filter by magnetic field effect.

Keywords: cascade optical fiber; finite element method; multimode interference; magneto-optical effect.

1 Introduction

Optical filters based on cascade (SMS) has considerable attention as a reliable optical device. The principle of the operation is based on the self- image and multimode interference (MMI) phenomena introduced by

✉ Shahad I Younus
140178@student.uotechnology.edu.iq
Anwaar A Al-Dergazly
aldergazly@gmail.com
A K Abass
abdulla.k.abass@uotechnology.edu.iq

1 Laser and Optoelectronic Engineering Department, University of Technology, Baghdad, Iraq,
2 Laser and Optoelectronic Engineering Department, Al-Naharain University, Baghdad, Iraq,

Soldano (Lucas B. Soldano and Erik C. M., 1995). The peak transmission wavelength shifts by external effect as strain, temperature, and external refractive index (ERI) change.

The structure is widely used as senor(Tian *et al.*, 2018, Zhang *et al.*, 2020, AL-Janaby and AL-Dergazly, 2020), fiber filter (Zhang et al. 2020, Álvarez-Tamayo *et al.*, 2016, Chakravarty *et al.*, 2017), recently, it is used as filter in CW optical parametric oscillation (OPO) cavity (Yu *et al.*, 2020, Tang *et al.*, 2019) since the nonlinear effect require low loss filter. The filter is used to tune Er (Khattak et al. 2018, Yuxin *et al.*, 2018, Walbaum and Fallnich, 2011) , Yb (Zhang *et al.*, 2012, Sánchez et al. 2006, Selvas et al. 2005), and Tm (X. Ma *et al.*, 2014, Li *et al.*, 2016, Zhang *et al.*, 2015) doped fiber laser due to that the cascade filter central wavelength can be modified to operate at any central wavelength. The tuning mechanism used in the mentioned systems either cumbersome or limited range. R Selvas et al. (Selvas et al. 2005) introduce the first Yb doped fiber laser tuned by MMI effect, the tuning structure consists of a SMF connected between an active Yb fiber and 105/125 MMF. The wavelength is selected by adjusting the separation between the MMF and a moving mirror (varying the MM section length), the tunability was 8 nm, and the output power was 500 mW. J. Sánchez et al. (Anzueto-Sánchez, et al. 2006) improved the mentioned mechanism by using a fiber mirror and a fiber gribber for simple alignment. The tunability was 12 nm. The previous mechanism is deviated from all fiber layout. T. Walbaum et al. (Walbaum and Fallnich, 2011) demonstrate a mode locked EDFL tuned by bending the SMS fiber filter, the obtained tunability was 11.6 nm. the pulse duration and the output power was 350 fs and 3.3 mW. L.Zhang et al. (Zhang *et al.*, 2012) used the SMS to tune the Yb doped fiber soliton laser at 1032 nm, the tunability obtained by stretching the MMF was 12 nm, the BW was 7.5 nm, the average delivered power was 31 mw with pulse duration 7 ps. X. Ma. et al. (X. Ma *et al.*, 2014) introduce a novel TDFL tuned by SNS filter covered with gradually altered liquid level, the NCF diameter was 200 µm, the 3 dB BW and the side mode suppression is 0.16 nm and 40 dB. P. Zhang et al. (Zhang *et al.*, 2015) propose a simple TDFL tuned by using SMS fiber structure. Three wavelength laser output is obtained. The tunability induced by applying a strain effect to change the MMF length using the polarization controller (PC) was 24 nm, the side mode suppression and the 3 dB BW was 54 dB and 0.04 nm. A. Khattak et al. (Khattak et al. 2018) used the SMS structure as a comb filter to obtain tunable and switchable, single and dual wavelength EDFL the tuning was 9.3 nm by modifying the PC. N. Li et al. (Li *et al.*, 2016) propose the largest tunable mode locked TDFL by using SMS filter with tunability about 100 nm by mechanical bending. Z. Yuxin et al. (Yuxin *et al.*, 2018) introduce EDFL tunable by a novel tapered large core 105/125 MMF between two SMF, the tunablility was 9 nm by mechanical bending, the 3 dB BW was 0.2 nm, the side mode suppression improved from 41 dB to 58 dB by using a taper. Applying mechanical effect as bending, strain, or stretching the fiber is endurable in long term operation. While tuning using liquid level is impractical as it required to locate the filter vertically and a motor is required to change the liquid level which complicate the system.

In this work, simple and novel fiber cascade (SNS) tunable filter by magnetic field effect numerically investigated by using finite element method. The transmission characteristics and the tuning properties of the filter with variable NCF dimension were studied and analyzed to optimize the filter performance. The tuning mechanism is based on surrounding the NCF with a magneto optical fluid (MOF), when the

magnetic field changed the RI of the MOF is varied cause a tuning to the peak transmission wavelength. Two materials were adopted for the study with different magneto-optic response. The device is highly stable, inexpensive, provide wide tuning range compared to other tuning methods. To the best of our knowledge, this is the first optical fiber MMI tunable filter by magnetic field effect.

2 Theory and Simulation

As stated by the theory of MMI (Lucas B. Soldano and Erik C. M., 1995, Guzman *et al.*, 2010, Younus et al. 2021), the transmitted wavelength can be given as

$$\lambda = \frac{n_{NCF} D^2}{L} P \quad (1)$$

Where n_{NCF}, D, and L is the NCF RI, diameter and length, P is an integer represents self-image order and $L = PZ_{self-image}$(Mukhopadhyay *et al.*, 2014), $Z_{self-image}$ is the distance of re-image. The peak wavelength shifts as the length, diameter or the RI is varied. The filter schematic is illustrated in

Fig 1, the structure consists of NCF connected between two SMF. The NCF RI is 1.444 while the SMF core/cladding RI and diameter is 1.444/1.423 and 8/125 µm. Using lower NCF diameter improve the Evanescent Wave (EW) (Wang *et al.*, 2011).

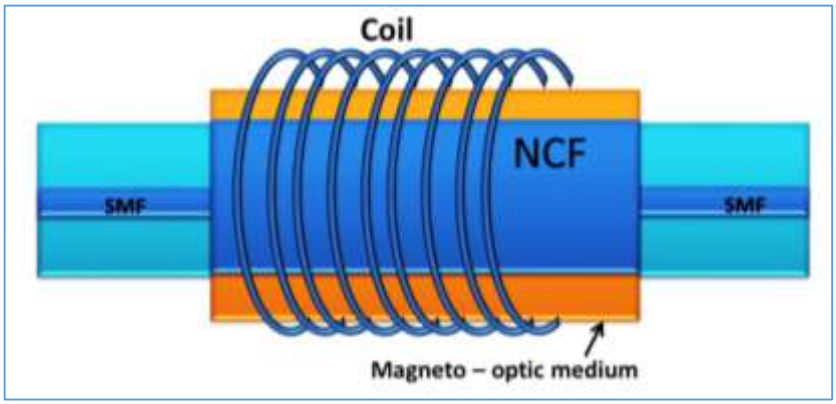

Fig 1 Schematic of the cascade optical fiber (SNS) tunable filter

The filter surrounded by a MOF, as the RI of the MOF is lower than that of the NCF the field guided by the total internal reflection and the Evanescent Field is produced at the interface between the NCF and the MOF, the field is penetrates inside the fluid to a specific depth (z) [(Raichlin and Katzir, 2008)]

$$z = \frac{\lambda}{2\pi n_{NCF} \sqrt{\sin^2 \vartheta - \left(\frac{n_2}{n_{NCF}}\right)^2}} \quad (2)$$

Where ϑ is the angle of incident, and n_2 is the RI of the MOF. This indicates the effective NCF diameter becomes (D+2Z), and the law of the MMI became(Antonio-Lopez *et al.*, 2010).

$$\lambda = \frac{n_{NCF}(D + 2Z)^2}{L} P \quad (3)$$

The MMI filter is placed in a MOF, the RI of the MOF varied with the magnetic field change, as the RI changed the penetration depth varied, as a result, the peak wavelength of the filter is tuned. The NCF length chosen precisely at the self-image point length to get a maximum transmission. Fourth self-image used in literature (Shulika, 2015) as lower attenuated self-image quality obtained. The NCF length influence the BW of the filter, as the length doubled or tripled the filter BW is narrowed. The relation is given as (Tripathi et al. 2010)

$$FWHM = 2\sqrt{\frac{\pi}{L}\left(\frac{d^2(\beta_0 - \beta_1)}{d\lambda^2}\right)^{-1}} \quad (4)$$

Where β_0 *and* β_1 is the propagation constant of the fundamental and first excited mode. The FEM simulation of the cascade fiber is performed in COMSOL multiphysics version 5.5, the same approach is used in the work (Younus et al. 2021) to numerically evaluate the field in the cascade fiber structure.

2. 1 Magneto-Optical Fluid

The tunable RI of the MOF with the magnetic field variation was utilized to shift the peak transmission of the SNS filter. As the string shape structures of the MOF are simply formed by the effect of the magnetic field, the RI of the MOF will modify with the change in the magnetic field as the micro-structure change of MOF would influence the RI. Fig 2 (a) show that RI of the 1st material Fe_3O_4 (Wang *et al.*, 2015) is 1.341 at 0 G, the RI is rise with the growing of the magnetic field, and it will saturate when magnetic field reaches 650 G at n =1.36. In Fig 2 (b), the 2nd material Fe_3O_4 (Bhatt and Patel, 2013) RI is 1.4 at 0 T, and reaches the saturation at n= 1.4639 when the magnetic field is 0.05 T (Bhatt and Patel, 2013).

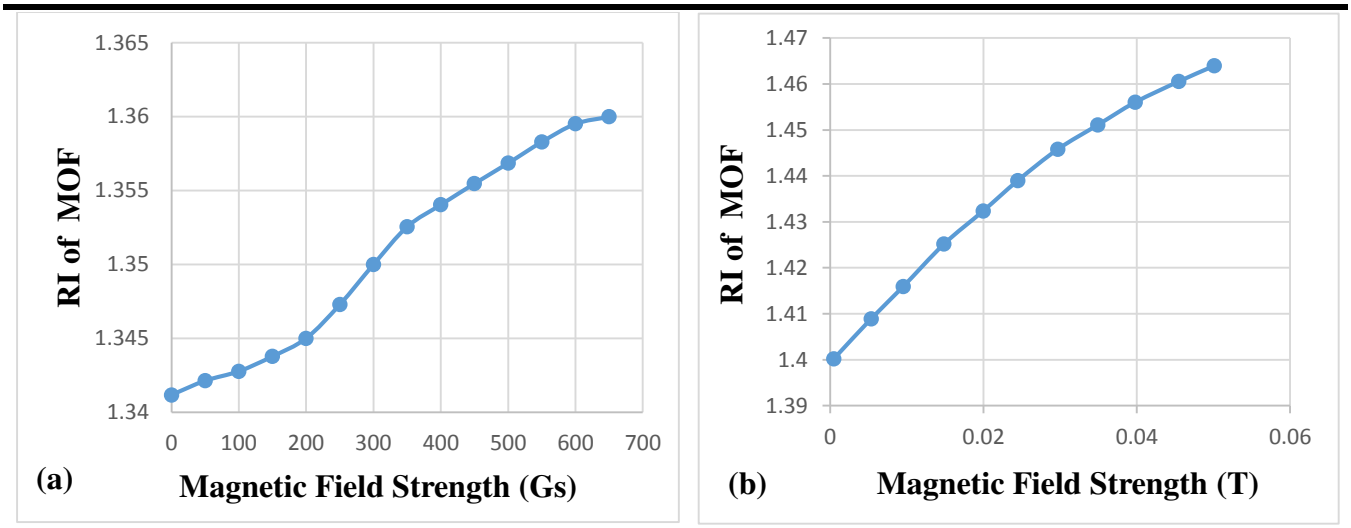

Fig 2 The MOF refractive index variation with the magnetic field strength (a) Fe_3O_4 (Wang *et al.*, 2015) (b) Fe_3O_4 (Bhatt and Patel, 2013).

3 Simulation Results and Discussion

3.1 The Transmission Characteristics at Variable NCF Dimension

In this section, the spectral response of the cascade (SNS) filter to the ERI change at variable NCF diameter and length was studied, the obtained optimized structure is used in the filter design.

3.1.1 NCF with Different Diameters

In this section, the cascade SNS structure simulated at NCF diameters from 50 to 200 µm, 25 µm step. The propagated field and the transmission spectrum were studied. The length of the NCF at the fourth self-image position determined and optimized to get a maximum transmission for each filter. In the Fig 3 (a) and Fig 4 (a), the field of the cascade structure for the 200 and 50 µm NCF diameter are simulated, the maximum transmission obtained at NCF lengths 14.952 and 0.945 cm, respectively, For ERI of the surrounding medium n_m=1 and wavelength 1.55 µm. Fig 3 (b) and Fig 4 (b) illustrate the shift in the peak wavelength by the ERI variation for the 200 and 50 µm NCF diameter, the studied ERI is 1, 1.33, 1.36, 1.4, and 1.44. For the 200 µm NCF diameter the studied spectral range is from 1540 to 1580 nm, the peak transmission is about 0.8 of the input intensity, the tunability and the FWHM are 15 and 6.8 nm. For the 50 µm NCF diameter, the studied spectral range from 1500 to 1650 nm, since the transmission spectrum is broad for the small NCF diameter. The tunability and the FWHM is 65 and 66 nm. The peak transmission is more than 0.95 of the input intensity. The difference in the peak transmitted intensity between the 200 and 50 μm NCF diameter is due to the increase in the number of the excited modes in large core size, not all the interfered modes in phase(Zhu *et al.*, 2008). At n_m=1.44 the field leak to the external medium, and the light is no longer confined in the fiber since the NCF RI is 1.444. The results for the studied structures are recorded in Table 1 and plotted in

Fig 5 The tunability and the FWHM variation with the NCF diameter, from the results, both the BW and the tunabitilty decrease with the increment in the NCF diameter. The reduction in the tunability is due to the depression in the penetration depth of the evanescent field as the core size increase. While the BW reduced due to the cutoff in high order modes (Pachon et al. 2012).

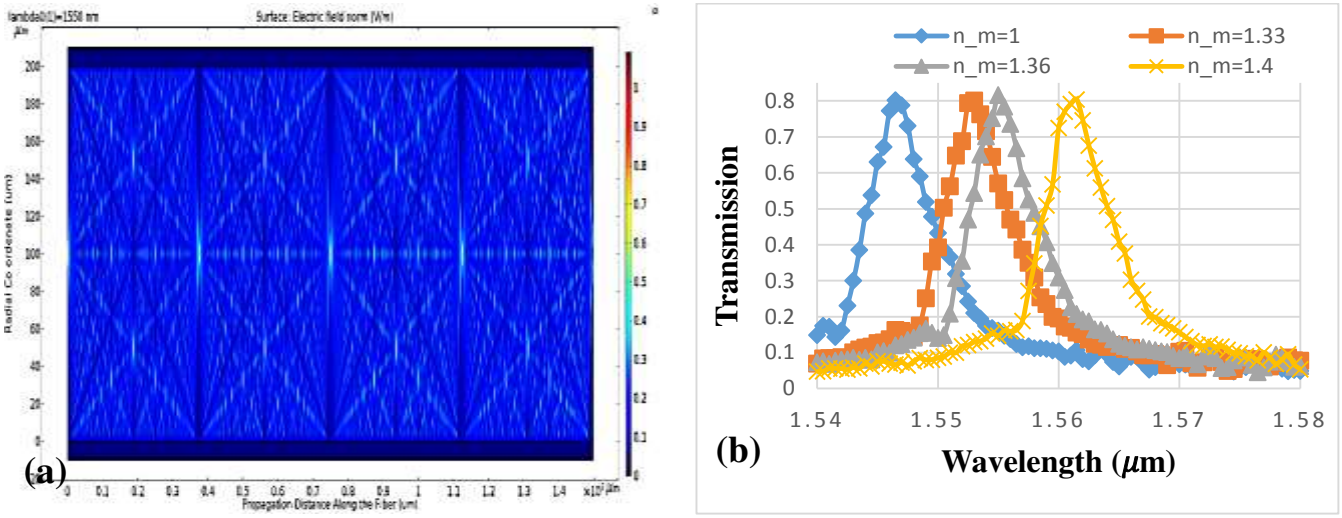

Fig 3 The cascade SNS structure field propagation (a) and the transmission spectrum (b) at 200 µm NCF diameter.

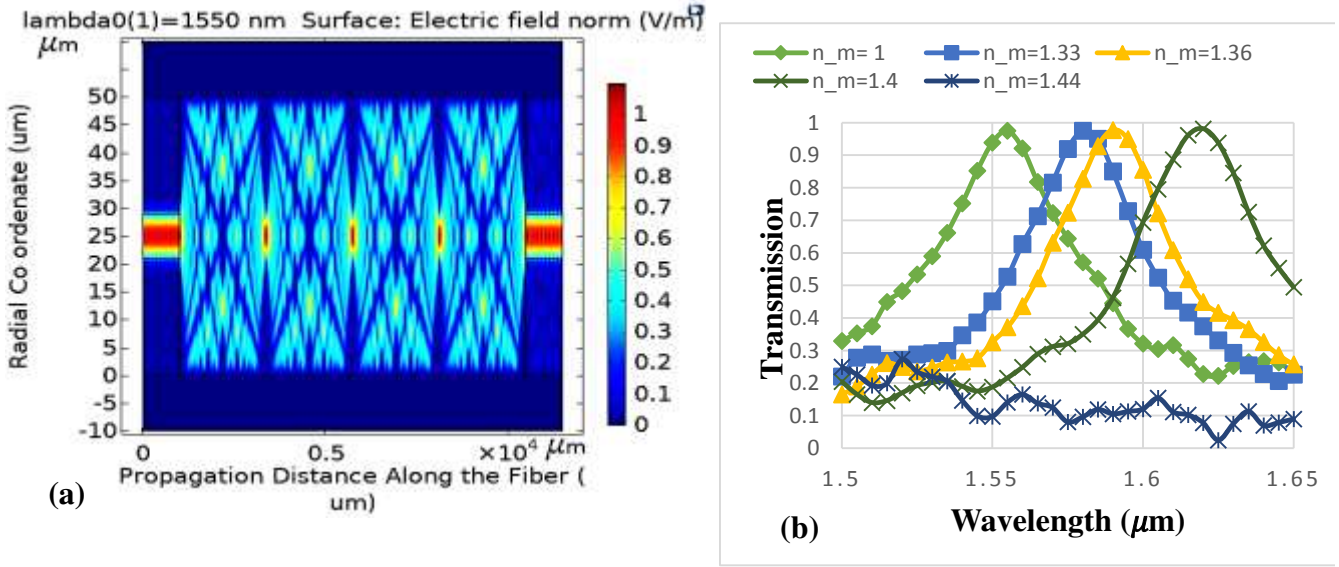

Fig 4 The cascade SNS structure field propagation (a) and the transmission spectrum (b) at 50 µm NCF diameter.

Table 1 The diameter and the corresponding NCF length of the fourth self–image, the FWHM and the tunability of the transmission at ERI between 1 to 1.4.

NCF Diameter (µm)	Fourth self-image Length of the NCF (cm)	FWHM (nm)	Tunability (nm)
50	0.945	66	65
75	2.118	30	40
100	3.754	17	31
125	5.85	11	25
150	8.42	7	20
175	11.45	6.8	17
200	14.952	6.4	15

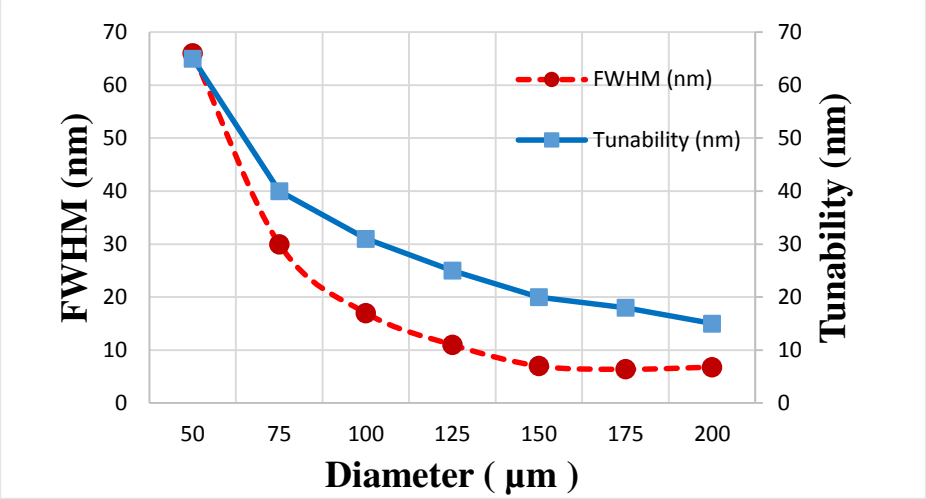

Fig 5 The tunability and the FWHM variation with the NCF diameter

3.1.2 NCF with Different Lengths

In this section, the transmission of the cascade structure at different NCF lengths is simulated. The lengths of the NCF is chosen to be equivalent to the self-image order (p) from 4 to 24, to study the variation in BW and tunability with different self-image order. The results show that the tunability is 65 nm for all the studied NCF lengths, and the transmission BW is reduced from 64 nm to 12 nm when the self-image order

varied from 4 to 24. The BW reduction illustrated in Fig 6, the self-image order (p) and its corresponding NCF length at 50 µm NCF diameter illustrated in Table 2 and plotted in Fig 7. The BW reduction with length is also illustrated in the work (Younus et al. 2021). The reduction in the BW occur due to the increase in the NCF length as in equation (4) of the relation between the BW and the midst fiber length. The peak wavelength remains the same since only (P) is the change in equation (1) of the MMI.

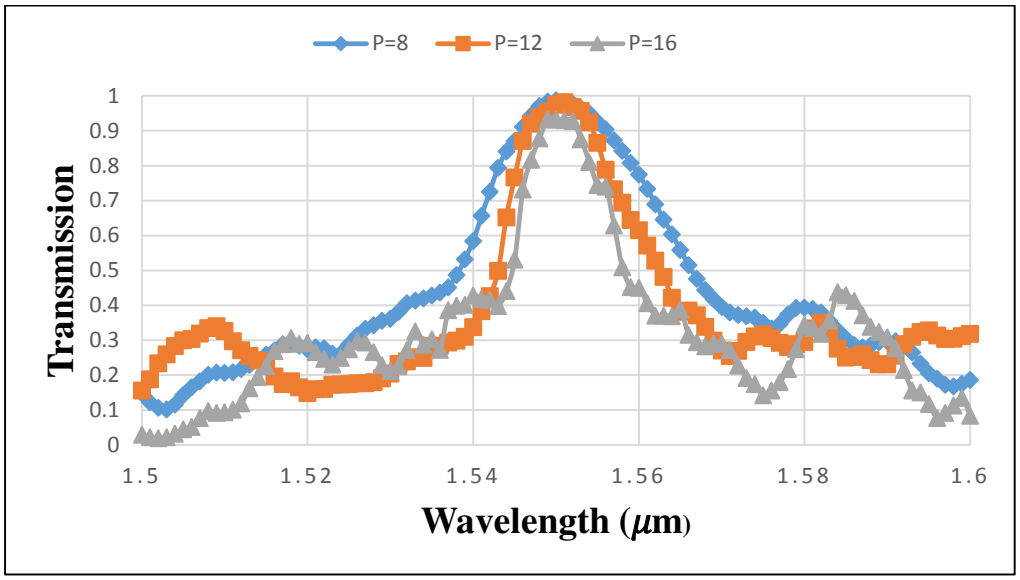

Fig 6 The transmission spectrum of the cascade structure at different self-image order.

Table 2 The self-image order and the corresponding NCF length, the FWHM and the tunability of the transmission at ERI between 1 to 1.44, the diameter of the NCF is 50 µm.

Self-image order (P)	NCF Length (cm)	FWHM (nm)	Tunability (nm)
4	0.947	64	65
8	1.894	28.1	65
10	2.3675	24	65
12	2.841	19.6	65
16	3.788	13.4	65
24	5.771	12	65

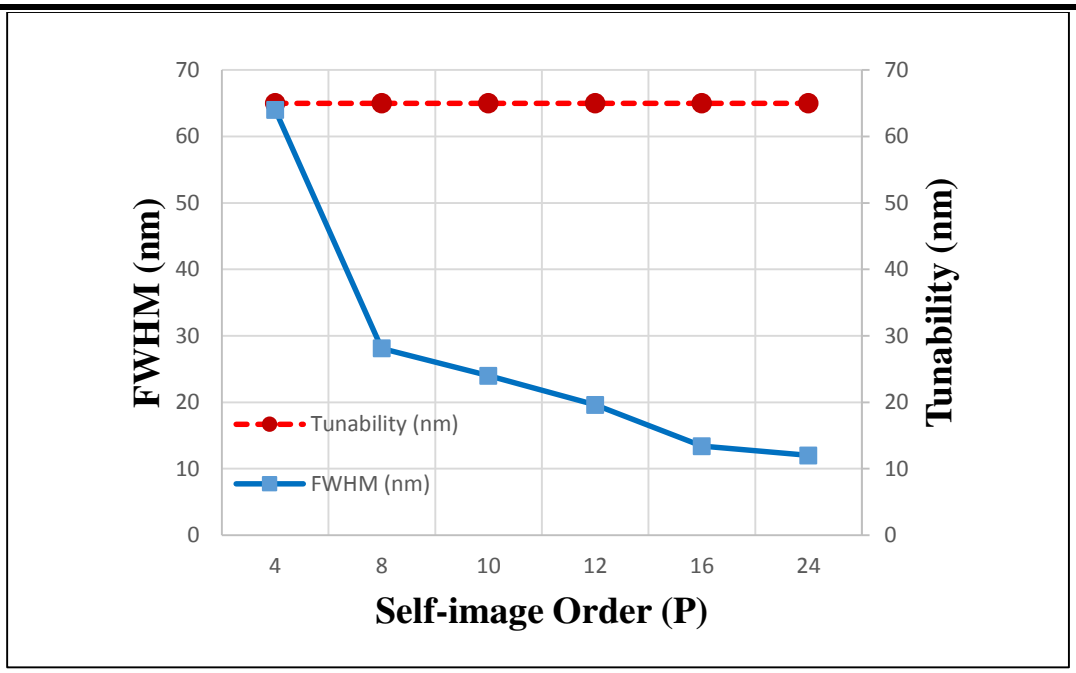

Fig 7 The tunability and the FWHM variation with the self-image order

3.2 Tunable Cascade Filter by Magnetic Field Effect

From section 3.1.1 and 3.1.2 to get high tunability and narrow BW it is recommended to use small NCF diameter with multi self-image order. In order to confirm the applicability of using the SNS structure as a filter tuned by magnetic field effect, two different materials with different magneto-optic response adopted Fig 2. The peak wavelength shifts via the variation in the RI of the MOF surrounding the NCF by the effect of the applied magnetic field. The filter performance optimized in the previous section, the NCF diameter is 50 µm and the length is 5.771 cm corresponding to 24 self-image order (P=24). For the first material, illustrated in Fig 8 (a), the obtained tunability is 6 nm from 1556 to 1562 nm, and the BW is 11.8 nm. The transmitted intensity about 0.9 of the input intensity. The response of the wavelength shifts to the magnetic field variation plotted in Fig 8 (b). For the second material, illustrated in Fig 9 (a), and due to a wide magneto-optic response of the MOF the tunability is 37 nm from 1518 to 1555 nm and the BW is 10.4 nm. The transmission about 0.98 of the input intensity except the last reading since the confinement reduced due to that the modes begin to leaks because the RI of the MOF is reaching the NCF RI, the peak wavelength response to the magnetic field variation is illustrated in Fig 9 (b). It is important to note that, when the filter inserted in the ring laser cavity, the BW will be reducing due to the wavelength feedback gain and loss supported by the loop of the ring cavity.

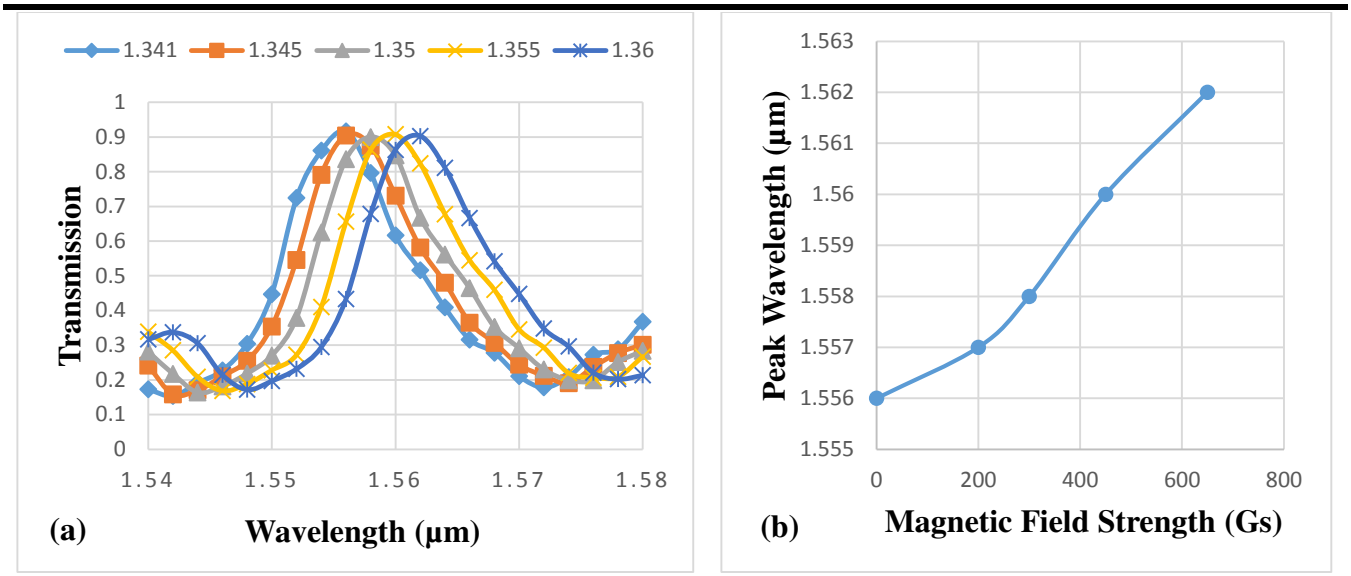

Fig 8 Tuning range of the cascade optical fiber (a) the peak wavelength shift as a function of the magnetic field strength (b)

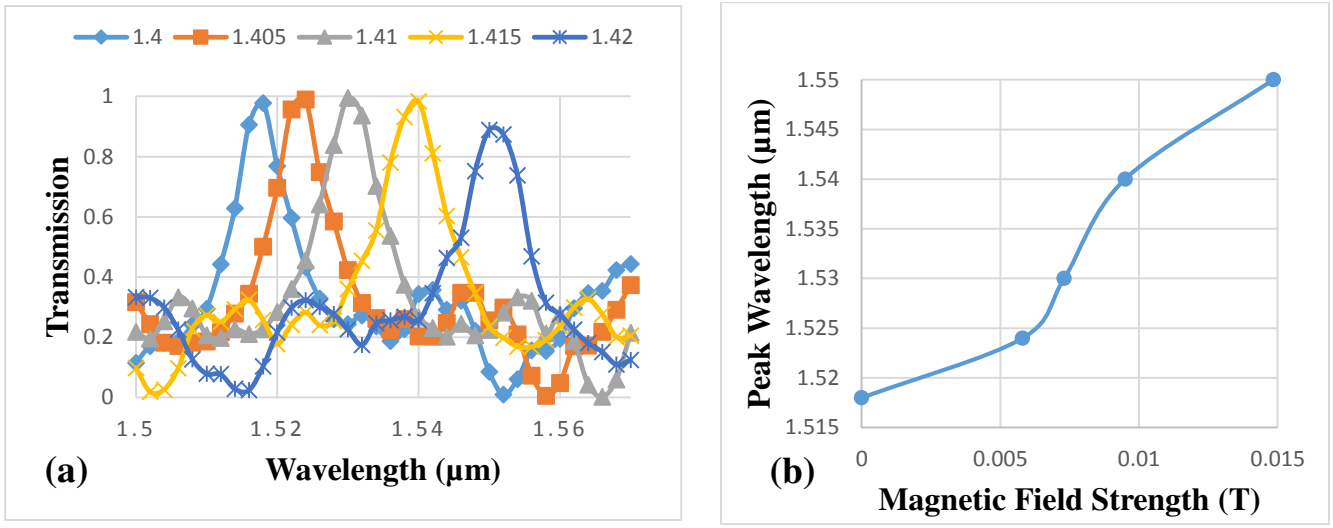

Fig 9 Tuning range of the cascade optical fiber (a) the peak wavelength shift as a function of the magnetic field strength (b)

Comparing the introduced MMI cascade tunable filter with other published literatures is carried out and the outcome is illustrated in Table 3. The introduced filter exhibits simple and reliable tuning mechanism with accepted tunability and BW. The tuning range is wider than in (Yu *et al.*, 2020), (L. Ma *et al.*, 2014) and (Li *et al.*, 2019).The tuning by mechanical bending and stretching in (Zhang et al. 2020), (Yu *et al.*, 2020) , and (Li *et al.*, 2019) is unreliable in long term operation. changing the level of the liquid in (X. Ma

et al., 2014) is impractical. While changing the liquid in (L. Ma *et al.*, 2014) required a large amount of different RI liquid. The proposed tuning mechanism can be enhanced by using wide magneto - optic material response and using NCF with high RI, which will perform in the next work.

Table 3 Comparison with tunable filters

Structure / MMF core diameter (µm)	**Tuning mechanism**	**Bandwidth (nm)**	**Tunable Range (nm)**	**Ref**
SMS/104	core offset and mechanical bending	FWHM-25	1954-1902 (52)	(Zhang, et al. 2020)
SMS/105	Stretching the structure	-	1642.5 - 1655.4 (12.9)	(Yu *et al.*, 2020)
SNGS	stretching the structure	-	1574 - 1601.1 (27.1)	(Li *et al.*, 2019)
SNS/200	Change of liquid level	3dB - 0.16	1818.52-1858.7 (45.18)	(X. Ma *et al.*, 2014)
SNS/104	RI	3dB - 0.02	1532-1564 (32)	(L. Ma *et al.*, 2014)
SNS/50	RI variation of the MOF by magnetic field effect	FWHM-11.6 FWHM-10.4	1556 - 1562 (6) 1518 - 1555 (37)	current work

4 Conclusion

Simple and novel cascade fiber (SNS) tunable filter by magnetic field effect is simulated using finite element method. The transmission characteristics and the tuning properties of the filter with variable NCF dimension and ERI are studied and analyzed to optimize the filter performance. Two materials were adopted for the study with different magneto-optic response. An improved filter performance obtained at 50 µm NCF diameter and 24 self-image order to get 37 nm tuning range with about 10 nm BW. The device is highly stable, inexpensive, provide wide tuning range compared with other tuning methods. This device can be use in optical communication, fiber sensor, spectroscopy, and in fiber laser technology. To the best of our knowledge, this is the first optical fiber MMI tunable filter by magnetic field effect.

References

AL-Janaby, N. and AL-Dergazly, A. (2020) 'Fabrication of multi-mode tip fiber sensor based on surface plasmon resonance (SPR)', *Sustainable Engineering and Innovation*, 2(1), pp. 10–17. doi: 10.37868/sei.v2i1.27.

Álvarez-Tamayo, R. I. *et al.* (2016) 'MMI filters configuration for dual-wavelength generation in a ring cavity erbium-doped fibre laser', *Journal of the European Optical Society*. Journal of the European Optical Society-Rapid Publications, 12(1). doi: 10.1186/s41476-016-0025-5.

Antonio-Lopez, J. E. *et al.* (2010) 'Tunable multimode-interference bandpass fiber filter', *Opt Lett*, 35(3), pp. 324-6 ST-Tunable multimode-interference bandpas. doi: 10.1364/OL.35.000324.

Anzueto-Sánchez, G., Martínez-Ríos, A., May-Arrioja, D. A., Torres-Gómez, I., Selvas-Aguilar, R., & Alvárez-Chávez, J. (2006) 'Enhanced tuning mechanism in fibre laser based on multimode interference effects', *ELECTRONICS LETTERS*, 42(23), pp. 487–489. doi: 10.1049/el.

Bhatt, H. and Patel, R. (2013) 'Optical Transport in Bidispersed Magnetic Colloids with Varying Refractive Index', *Journal of Nanofluids*, 2(3), pp. 188–193. doi: 10.1166/jon.2013.1058.

Castillo-Guzman, A. *et al.* (2010) 'Widely tunable Erbium-doped fiber laser based on multimode interference effect', *OSA*. doi: 10.1364/cleo.2009.jtud62.

Chakravarty, U. *et al.* (2017) 'Narrow-linewidth broadly tunable Yb-doped Q-switched fiber laser using multimode interference filter', *Applied Optics*. doi: 10.1364/ao.56.003783.

Khattak, A., Tatel, G. and Wei, L. (2018) 'Tunable and Switchable Erbium-Doped Fiber Laser Using a Multimode-Fiber Based Filter', *Applied Sciences*, 8(7), p. 1135. doi: 10.3390/app8071135.

Li, L. *et al.* (2019) 'L-Band Tunable and Dual-Wavelength Mode-Locked Fiber Laser with NCF-GIMF-Based SA', *IEEE Photonics Technology Letters*. IEEE, 31(8), pp. 647–650. doi: 10.1109/LPT.2019.2905149.

Li, N. *et al.* (2016) 'All-fiber widely tunable mode-locked thulium-doped laser using a curvature multimode interference filter', *Laser Physics Letters*, 13(7). doi: 10.1088/1612-2011/13/7/075103.

Lucas B. Soldano and Erik C. M. (1995) 'Optical Multi-Mode Interference Devices Based on Self-Imaging : Principles and Applications', *Journal of Lightwave Technology*, 13, p. 615. doi: 10.1049/iet-opt.2010.0106.

Ma, L. *et al.* (2014) 'Tunable fiber laser based on the refractive index characteristic of MMI effects', *Optics and Laser Technology*. Elsevier, 57, pp. 96–99. doi: 10.1016/j.optlastec.2013.10.001.

Ma, X. *et al.* (2014) 'Widely tunable thulium-doped fiber laser based on multimode interference with a large No-core fiber', *Journal of Lightwave Technology*. doi: 10.1109/JLT.2014.2342251.

Mukhopadhyay, P. K. *et al.* (2014) 'Note: Broadly tunable all-fiber ytterbium laser with 0.05 nm spectral width based on multimode interference filter', *Review of Scientific Instruments*, 85(5), pp. 34–37. doi: 10.1063/1.4874746.

Oleksiy Shulika, I. S. (2015) *Advanced Lasers Laser Physics and Technology for Applied and Fundamental Science*, *springer*. doi: 10.1002/aja.1000300204.

Pachon, E. G. P., Franco, M. A. R. and Cordeiro, C. M. B. (2012) 'Spectral bandwidth analysis of high sensitivity refractive index sensor based on multimode interference fiber device', *OFS2012 22nd International Conference on Optical Fiber Sensors*, 8421(October), pp. 84217Q-84217Q–4. doi: 10.1117/12.969928.

Raichlin, Y. and Katzir, A. (2008) 'Fiber-optic evanescent wave spectroscopy in the middle infrared', *Applied Spectroscopy*, 62(2). doi: 10.1366/000370208783575456.

Saurabh Mani Tripathi, Arun Kumar, Emmanuel Marin, J.-P. M. (2010) 'Single-Multi-Single Mode Structure Based Band Pass / Stop Fiber Optic Filter With Tunable Bandwidth', *Journal of Lightwave Technology Institute of Electrical and Electronics Engineers (IEEE)/Optical Society of America(OSA)*, 28(24), p. .3535-3541.

Selvas, R., Torres-Gomez, I. and Martinez-Rios, A. (2005) 'Wavelength tuning of fiber lasers using multimode interference effects', *Osa*, 13(23), pp. 9439–45. doi: Article.

Tang, Z. *et al.* (2019) 'Tunable CW All-fiber optical parametric oscillator based on the cascaded single-mode-multimode-single-mode fiber structures', *SPIE*, (March 2019), p. 66. doi: 10.1117/12.2509665.

Tian, K. *et al.* (2018) 'High sensitivity temperature sensor based on singlemode-no-core-singlemode fibre structure and alcohol', *Sensors and Actuators, A: Physical*, 284(October), pp. 28–34. doi: 10.1016/j.sna.2018.10.016.

Walbaum, T. and Fallnich, C. (2011) 'Multimode interference filter for tuning of a mode-locked all-fiber erbium laser', *Optics Letters*, 36(13), p. 2459. doi: 10.1364/ol.36.002459.

Wang, P. *et al.* (2011) 'High-sensitivity , evanescent field refractometric sensor based on a tapered , multimode fiber interference', *OPTICS LETTERS*, 36(12), pp. 10–13. doi: 10.1364/OL.36.002233.

Wang, Q. *et al.* (2015) 'Magnetic field sensing based on fiber loop ring-down spectroscopy and etched fiber interacting with magnetic fluid', *Optics Communications*. Elsevier, 356, pp. 628–633. doi: 10.1016/j.optcom.2015.08.043.

Younus, S. I., Al-Dergazly, A. A. and Abass, A. K. (2021) 'Characterization of Multimode Interference Based Optical Fiber', *IOP Conference Series: Materials Science and Engineering*, 1076(1), p. 012060. doi: 10.1088/1757-899x/1076/1/012060.

Yu, J. *et al.* (2020) 'All-fiber CW optical parametric oscillator tuned from 1642.5 to 1655.4 nm by a low-loss SMS filter', *Results in Physics*. Elsevier, 17(April), p. 103136. doi: 10.1016/j.rinp.2020.103136.

Yuxin, Z. *et al.* (2018) 'Tunable single-wavelength erbium-doped fiber ring laser using a large-core fiber', *Infrared Physics and Technology*. doi: 10.1016/j.infrared.2018.09.030.

Zhang, F. *et al.* (2020) 'A refractive index sensitive liquid level monitoring sensor based on multimode interference', *Photonics*, 7(4), pp. 1–10. doi: 10.3390/photonics7040089.

Zhang, K., Alamgir, I. and Rochette, M. (2020) 'Midinfrared Compatible Tunable Bandpass Filter Based on Multimode Interference in Chalcogenide Fiber', *Journal of Lightwave Technology*. IEEE, 38(4), pp. 857–863. doi: 10.1109/JLT.2019.2948109.

Zhang, L. *et al.* (2012) 'Tunable all-fiber dissipative-soliton laser with a multimode interference filter', *Optics Letters*, 37(18), p. 3828. doi: 10.1364/ol.37.003828.

Zhang, P. *et al.* (2015) 'Tunable multiwavelength Tm-doped fiber laser based on the multimode interference effect', *Applied Optics*, 54(15), p. 4667. doi: 10.1364/ao.54.004667.

Zhu, X. *et al.* (2008) 'Detailed investigation of self-imaging in largecore multimode optical fibers for application in fiber lasers and amplifiers', *Optics Express*, 16(21), p. 16632. doi: 10.1364/oe.16.016632.